

On the waiting time distributions of systems of locally confined particles with rare interactions

Thomas Gilbert

Center for Nonlinear Phenomena and Complex Systems, Université Libre de Bruxelles, C.P. 231, Campus Plaine, B-1050 Brussels, Belgium
E-mail: thomas.gilbert@ulb.ac.be

Received 9 May 2011

Accepted 6 June 2011

Published 22 June 2011

Online at stacks.iop.org/JSTAT/2011/P06015

[doi:10.1088/1742-5468/2011/06/P06015](https://doi.org/10.1088/1742-5468/2011/06/P06015)

Abstract. We report on the computation of the waiting time distributions of different model systems of locally confined particles subject to rare hard-core interactions. These distributions are numerically found to fall off fast, in particular when the timescales that characterize the interactions among particles in neighbouring traps are well separated from the timescales that characterize the motion of particles within their confining cells. Our findings leave open the possibility that the waiting time distributions of systems with a polygonal trapping mechanism display algebraic tails but otherwise refute the arguments of Lefevre *et al* (2010 *J. Stat. Mech.* L12004) according to which such algebraic tails occur systematically. Where it is observed, the algebraic decay is, in any case, much faster than predicted by these authors.

Keywords: transport processes/heat transfer (theory), current fluctuations

Contents

1. Introduction	2
2. Stochastic energy exchanges	4
3. Models of interacting particles with local confinement rules	6
3.1. A two-dimensional dispersing billiard table	7
3.2. A three-dimensional semi-dispersing billiard table	9
3.3. Two- and three-dimensional semi-defocusing billiard tables	11
4. Conclusions	13
Acknowledgments	14
References	14

1. Introduction

According to the authors of [1] (denoted LMZ below), the energy current of a large class of models of locally confined billiard particles in interaction is carried from cell to cell by particles which may have arbitrary low energies with sufficiently large probabilities, a property which manifests itself in the algebraic tails of the waiting time distribution—that is, the distribution of times that separate successive collision events between a given particle and its neighbours. This postulate further leads these authors to conclude that the thermodynamic potential describing the macroscopic fluctuations of the current and local energy of such systems is neither analytic nor strictly convex.

We argue that this conclusion is, in fact, based on a flawed assumption which ignores both the dimensionality of the dynamics underlying the process of energy transfer in said models, as well as the effect of correlations between the different components of the system. We further stress the crucial role played by the assumption of separation of timescales, under which these models undergo an effective factorization of their nonequilibrium energy distributions into products of single-cell distributions.

The systems under consideration consist of a class of materials in which gas particles are trapped in a solid nanoporous matrix in such a way that collisions with the walls of the nanopores occur more frequently than collisions among gas particles. If we ignore the possibility of energy transfer between gas particles and the solid matrix and make the assumption that the size of the nanopores is small enough to prevent gas particles from moving through them and yet large enough that interactions seldom take place among the gas particles belonging to neighbouring nanopores, we obtain a class of models where thermalization takes place in two stages: (i) the first, on a fast scale, is a stage of local thermalization driven by the wall collision events and the local mixing within separate nanopores and (ii) a second stage of thermalization among neighbouring nanopores, which takes place through binary collision events, i.e. collisions between two gas particles

belonging to neighbouring nanopores. By controlling the ratio between the frequency of such events and that of wall collision events, we can ensure the completion of stage (i) before stage (ii) takes place.

In this regime where the separation of timescales between wall and binary collision events is effective, one finds that the heat conductivity reduces, up to a dimensional factor, to the frequency of binary collision events. The same result is obtained assuming local thermalization, which amounts to an exact factorization of the phase-space distribution into products of single-cell distributions at local thermal equilibrium [2, 3]. In practice, one considers a collection of cells aligned along a horizontal axis, each containing a single trapped particle. By thermalizing the walls of the left and rightmost cells at two distinct temperatures T_L and T_R , a thermalization of the gas particles trapped within these two cells is achieved on a timescale much faster than that of binary collision events. The resulting temperature gradient between the two ends of the system induces a heat current, carried through energy exchanges between the thermalized particles and the particles trapped in the bulk. The relation of the heat current to the fixed temperature gradient, $T_R - T_L$, yields, in the large system size limit, the heat conductivity. By tuning the system's parameters towards a critical geometry where energy exchanges become impossible, the separation of timescales between wall and binary collision events becomes effective and the ratio of heat conductivity to frequency of binary collisions goes to unity.

The combination of separation of timescales and large system sizes imposes obvious limitations on the numerical implementation of such a scheme. A workaround is therefore desirable. Assuming an effective thermalization, we thus think of a large system as composed of many independent units, in which a single particle interacts with two particles thermalized at close but different temperatures (this thermalization occurs in the usual way through wall collision events). The properties of such a system were investigated in [4].

Similar considerations led LMZ to introduce a single-cell model, where a particle rattles about a square cell, whose left and right walls are thermalized at fixed temperatures, and no other form of interaction takes place. The obvious trouble with this model is that it does not differentiate between wall and binary collision events, thereby losing much of the physics of the rarely interacting particle models under consideration. These authors further argue that a single dimension is relevant to the transport of heat in these models and thus reduce their model system to a one-dimensional particle bouncing back and forth between the two thermalized ends of an interval.

But dimensionality does matter. Indeed, as is the case with the mechanical models displayed in figures 2, 5 and 6 below, energy transfers take place through binary collision events between discs or spheres, which are otherwise confined to semi-dispersing [2, 4] or polygonal billiard cells [3]. An elastic collision that takes place between two neighbouring particles affects only one out of their two or three velocity components. The amount of energy that is exchanged in this process is therefore, on average, only a half or a third of the total amount of kinetic energy carried by each of the two colliding particles. The important implication of this elementary fact is that the probability that a particle may have arbitrary low energy is, in fact, much smaller than LMZ had contemplated. It should therefore be clear that the sequence of waiting times of the systems of rarely interacting particles under investigation will not be distributed according to the waiting time distribution of the successive collisions of the one-dimensional bouncing ball model,

which is

$$\psi_{1D}(t) = \frac{2}{\pi t^3} e^{-1/\pi t^2}, \quad (1)$$

here normalized so that the average time between bounces is unity.

Our purpose is to elucidate what the waiting time distributions of systems of locally confined particles actually are.

In section 2, we discuss the properties of systems of stochastic energy exchanges, modelled on the collisional dynamics of particles separately confined either to two-dimensional dispersing cells [5] or to three-dimensional dispersing or semi-dispersing cells [6]. Using generic properties of these models, we propose a simple characterization of their waiting time distributions, according to which we infer algebraic decay of their tails with exponents 7 and 10, for two- and three-dimensional dynamics respectively, to be contrasted with 3 in equation (1). We further argue that these values do not correctly account for correlation effects which remove these tails, as shown by direct numerical computations of the corresponding quantities. Instead, our numerical findings are consistent with exponential tails.

In section 3 we turn to actual billiard models and present numerical computations of their waiting time distributions as a parameter controlling the separation of timescales with wall and binary collision events is varied. In sections 3.1 and 3.2, we provide numerical evidence to the effect that the results obtained for the stochastic energy exchange models carry over to the billiard dynamics from which they derive. In section 3.3, we consider systems of particles confined to polygonal cells and report numerical results showing their waiting time distributions have scalings different from the previous models, with a common algebraic tail exponent close to seven, irrespective of the dimensionality of the cells. Accordingly, the validity of the conclusions drawn by LMZ is limited to the special class of systems with polygonal trapping mechanism.

2. Stochastic energy exchanges

When the confining dynamics of individual particles consist of dispersive or semi-dispersive billiards, the energy exchanges of rarely interacting particle systems can be brought down to stochastic energy exchange systems [4]. Given a lattice of N cells with a configuration $\{\epsilon_1, \dots, \epsilon_N\}$ of local energy variables, this is to say their time-dependent distribution $P_N(\epsilon_1, \dots, \epsilon_N, t)$ evolves according to the master equation

$$\begin{aligned} \partial_t P_N(\epsilon_1, \dots, \epsilon_N, t) = & \frac{1}{2} \sum_{a,b=1}^N \int d\eta [W(\epsilon_a + \eta, \epsilon_b - \eta | \epsilon_a, \epsilon_b) P_N(\dots, \epsilon_a + \eta, \dots, \epsilon_b - \eta, \dots, t) \\ & - W(\epsilon_a, \epsilon_b | \epsilon_a - \eta, \epsilon_b + \eta) P_N(\dots, \epsilon_a, \dots, \epsilon_b, \dots, t)], \end{aligned} \quad (2)$$

whose stochastic kernel W , which specifies the process of energy exchange η between the two neighbouring cells a and b with respective energy variables ϵ_a and ϵ_b , $-\epsilon_b \leq \eta \leq \epsilon_a$, depends solely on the dimensionality of the underlying collision process among hard spheres or discs, not on the geometry of the confining cell [5, 6].

The exponential rate at which two neighbouring cells at fixed energies ϵ_a and ϵ_b exchange energy is the energy exchange frequency:

$$\nu(\epsilon_a, \epsilon_b) = \int d\eta W(\epsilon_a, \epsilon_b | \epsilon_a - \eta, \epsilon_b + \eta), \quad (3)$$

which has the universal property that it is a homogeneous function of degree 1/2, namely

$$\nu(\alpha\epsilon_a, \alpha\epsilon_b) = \sqrt{\alpha}\nu(\epsilon_a, \epsilon_b). \quad (4)$$

We refer to [5, 6] for the expressions of W and ν , respectively, corresponding to two- and three-dimensional underlying dynamics.

With the energy exchange frequencies (3), we can write down the waiting time distribution of the system of N fluctuating energy cells. Assuming an equilibrium state with constant total energy E and periodic boundary conditions (identifying cells 1 and $N + 1$), this is the distribution

$$\psi_{2D}^{\text{mic}}(t) = \frac{N!}{E^{N-1}} \int d\epsilon_1 \cdots d\epsilon_N \sum_{i=1}^N \nu(\epsilon_i, \epsilon_{i+1}) \exp \left[-t \sum_{i=1}^N \nu(\epsilon_i, \epsilon_{i+1}) \right] \delta(\epsilon_1 + \cdots + \epsilon_N - E), \quad (5)$$

which yields the probability that the next energy exchange (regardless of where in the system it takes place) will occur at time t . In the spirit of LMZ, we would like to define the waiting time of a given energy cell in this system, irrespective of the others. A reasonable way would be to consider equation (5) with $N \rightarrow \infty$, let $E/N \equiv k_B T$ constant, and simply assume that any given cell will be updated at a rate $2/N$ that of (5). The corresponding distribution would clearly be exponential.

A different, and rather naive way as it turns out, is to consider instead a system in canonical equilibrium, say at unit temperature, and write down the waiting time distributions as expectation values of the exponential renewal rates with respect to the canonical equilibrium distributions. Assuming a one-dimensional array of cells, the waiting time distributions of a cell at fluctuating energy ϵ surrounded by two neighbouring cells at respective fluctuating energies ϵ_L and ϵ_R would thus reduce to the expressions

$$\psi_{2D}(t) = \int d\epsilon_L d\epsilon_R d\epsilon [\nu(\epsilon_L, \epsilon) + \nu(\epsilon_R, \epsilon)] \exp \{ -t[\nu(\epsilon_L, \epsilon) + \nu(\epsilon_R, \epsilon)] - \epsilon_L - \epsilon - \epsilon_R \}, \quad (6)$$

in the case of two-dimensional underlying dynamics, or

$$\begin{aligned} \psi_{3D}(t) &= \frac{4}{\pi} \int d\epsilon_L d\epsilon_R d\epsilon \sqrt{\epsilon_L \epsilon_R} \epsilon [\nu(\epsilon_L, \epsilon) + \nu(\epsilon_R, \epsilon)] \\ &\quad \times \exp \{ -t[\nu(\epsilon_L, \epsilon) + \nu(\epsilon_R, \epsilon)] - \epsilon_L - \epsilon - \epsilon_R \}, \end{aligned} \quad (7)$$

in the case of three-dimensional underlying dynamics.

Equations (6) and (7) are easily adapted to other lattice configurations, such as a two-dimensional square lattice (in which case four neighbouring cells should be considered) or a three-dimensional cubic lattice (with six neighbouring cells). Without attempting to carry out these integrals explicitly, it is straightforward to extract their long-time decay

rates using equation (4), which turn out to be algebraic:

$$\psi_{2D}(t) \stackrel{t \rightarrow \infty}{\sim} t^{-7}, \quad \psi_{3D}(t) \stackrel{t \rightarrow \infty}{\sim} t^{-10}, \quad (8)$$

with every additional neighbouring cell bringing in another power t^{-2} or t^{-3} , depending on the dimensionality, two or three, of the underlying dynamics. Equation (8) is in sharp contrast with the algebraic decay exponent three of the waiting time distribution (1) proposed by LMZ.

In comparison to equation (1), equations (6) and (7) would seem better guesses, but are nevertheless incorrect. The reason is there is no simple prescription for disentangling the waiting times of the different components of a larger system the way we just did, which was to ignore their interactions with other neighbours. We should rather consider the equivalent of the distribution $\psi_{2D}^{\text{mic}}(t)$, equation (5), for a large system with two thermal baths at its ends:

$$\begin{aligned} \psi_{2D}^{\text{can}}(t) = & \int d\epsilon_L d\epsilon_1 \cdots d\epsilon_N d\epsilon_R \left[2\nu_B + \sum_{i=1}^N \nu(\epsilon_i, \epsilon_{i+1}) \right] \\ & \times \exp \left\{ -t \left[2\nu_B + \sum_{i=1}^N \nu(\epsilon_i, \epsilon_{i+1}) \right] - \epsilon_L - \epsilon_1 - \cdots - \epsilon_N - \epsilon_R \right\}, \end{aligned} \quad (9)$$

where ν_B denotes the constant frequency at which the energy of the thermalized cells gets renewed, and scale it in a way similar to that described above to obtain the single-cell waiting time distribution. The result would again be an exponential distribution.

We resort to numerical computations in order to separate thermalizing events from energy exchanges. In figure 1(a), we plot the waiting time distributions corresponding to energy exchange events of the middle cell of a system of three cells, with both left and right neighbours thermalized at unit temperature. The renewal frequencies ν_B of the thermalized cells were here set to unity, which is enough to efficiently thermalize the systems; the first four moments of the single-cell energy distributions were checked to be within three digits of their canonical expectation values, $\langle \epsilon^n \rangle = n!$ in the case of two-dimensional underlying dynamics or $\langle \epsilon^n \rangle = 2^{-n}(2n+1)!!$ for the three-dimensional case.

The figures display histograms of the waiting times for both two-dimensional (left panel) and three-dimensional (right panel) underlying dynamics, collected over 10^8 and 10^9 events, respectively. Also shown is a comparison with numerical computations of equations (6) and (7), respectively. These results clearly establish that the waiting time distributions decay faster than predicted by equation (8). As shown in the insets, their tails are, in fact, well fitted by exponential laws.

Similar results were obtained for larger system sizes, for example in figure 1(b) where we show the waiting time distribution of the middle cell of systems of 22 cells with thermalization at unit temperature carried out at rates $\nu_B = 10$ in cells 1 and 22.

3. Models of interacting particles with local confinement rules

In this section, we examine the waiting time distributions of actual billiard models of systems of separately confined particles with rare interactions. We consider four different

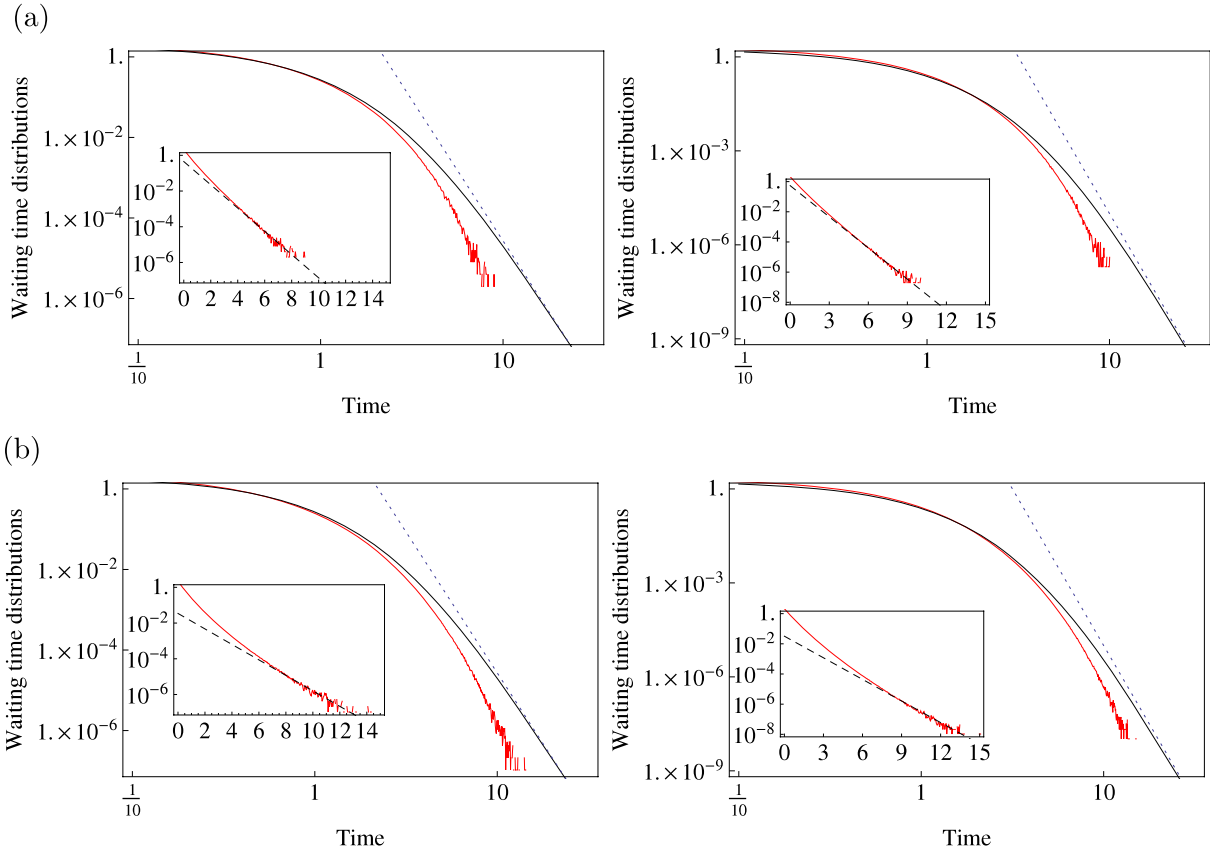


Figure 1. Numerical computation of the waiting time distributions of the middle cell of stochastic energy exchange systems of respectively (a) a system of a single cell in contact with two thermalized cells and (b) a system of 20 aligned cells with its two ends in contact with thermalized cells, aligned on a one-dimensional lattice, with left and rightmost cells thermalized to unit temperature at constant unit rates. The left panels correspond to two-dimensional underlying dynamics and the right panels to three-dimensional underlying dynamics. In each figure, a numerical computation of equations (6) (left panel) and (7) (right panel) is shown for comparison (solid line); the dotted lines show the tails (8).

examples. The first two are examples of systems with (two-dimensional) dispersing and (three-dimensional) semi-dispersing confining dynamics and thus reduce, under the assumption of the loss of memory effects as a control parameter is decreased towards a critical value, to the stochastic energy exchange models whose waiting time distributions were studied in section 2. The remaining two models, on the other hand, have confining mechanisms of polygonal billiard type and are therefore not amenable to a similar treatment. As detailed below, numerical evidence suggests these polygonal models both have waiting time distributions with algebraic tails with exponents close to seven.

3.1. A two-dimensional dispersing billiard table

The first model we consider is a two-dimensional lattice billiard, as introduced in [4], and is sketched in figure 2. It consists of a lattice of three rhombic-shaped cells of sides $l = 1/\sqrt{2}$, with fixed discs of radius ρ_f at their edges and a single disc of radius ρ_m

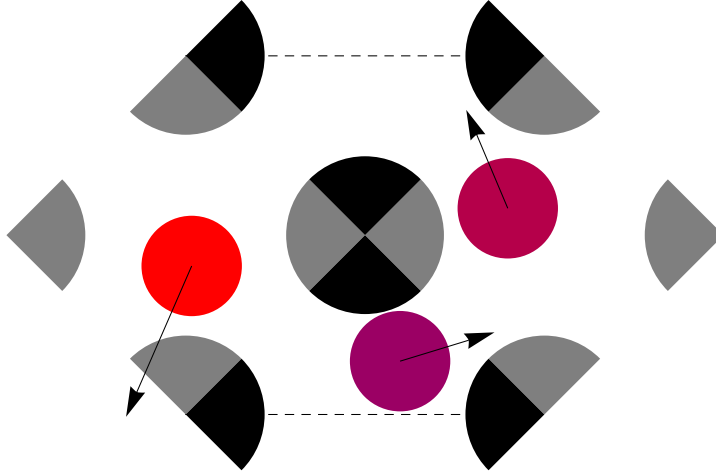


Figure 2. Two-dimensional lattice billiard with rhombic tiling. The walls of the left and right cells (in grey) are thermalized to unit temperatures. The horizontal lines in the middle cell indicate periodic boundary conditions. The particle in the middle cell is subjected to the usual rules of elastic collisions when it collides with the fixed discs at the four corners of the cell, or with the moving particles in the neighbouring cells.

trapped inside them. The system is conveniently characterized in terms of two parameters, $\rho \equiv \rho_m + \rho_f$, which fixes the geometry of isolated cells and is chosen so particles are trapped inside the non-empty area at the cell centre, $l/2 < \rho < l/\sqrt{2}$, and ρ_m , with $\rho_c \equiv \sqrt{\rho^2 - l^2/4} < \rho_m < \rho$, the lower limit corresponding to the critical value of the radius of the moving discs below which energy-exchanging collisions are impossible. Having fixed the parameter ρ , which controls wall collision events, we vary the parameter ρ_m and decrease its value towards ρ_c to control the separation of timescales, $\nu_B \ll \nu_W$.

The walls inside the left and rightmost cells are thermalized at unit temperatures so that, when the corresponding particles collide with these walls, they get reflected with normal and tangential components fixed according to the usual rules of thermal wall simulation [7].

Numerical simulations of this model were performed with $\rho = 9/25$ (for which $\rho_c \simeq 0.07$) and taking ρ_m as small as 0.09. We checked that the particles had reached a canonical equilibrium distribution by computing the first few moments of the energy distributions in each individual cell and verified $\langle \epsilon^n \rangle = n!$ within three to four digits of accuracy, for n up to four.

A computation of the time elapsed between successive binary collisions (or waiting times) yielded the frequency of binary collisions ν_B , which we compared to the frequency of wall collisions in the absence of interaction between the neighbouring particles¹

$$\nu_W = \bar{v} \frac{|\partial \mathcal{B}_\rho|}{\pi |\mathcal{B}_\rho|}, \quad (10)$$

¹ Equation (10) applies to two-dimensional billiards. A slightly modified formula:

$$\nu_W = \bar{v} \frac{|\partial \mathcal{B}_\rho|}{4 |\mathcal{B}_\rho|},$$

applies to three-dimensional billiards [8], in which case we have the canonical average speed $\bar{v} = \sqrt{8/\pi}$.

where $\bar{v} = \sqrt{\pi/2}$ is the average speed in the two-dimensional canonical ensemble at a temperature of unity, $|\mathcal{B}_\rho|$ denotes the area of the billiard cell and $|\partial\mathcal{B}_\rho|$ its perimeter. The results of this comparison as the parameter ρ_m is varied are displayed in the left panel of figure 3(a) and allow the effectiveness of the separation of timescales, $\nu_B \ll \nu_W$, to be assessed.

The waiting times statistics of the middle particle interacting with its two thermalized neighbours are shown for several values of the parameter ρ_m in the right panel of figure 3(a). These distributions were evaluated by computing histograms² of the times separating successive binary collision events of this particle with its two neighbours, thermalized through wall interactions. Much as with the corresponding two-dimensional stochastic model discussed in section 2, the results clearly show a decay faster than the algebraic decay predicted by (8). The tails of the computed distributions are, in fact, well approximated by exponentials, even as $\rho_m \rightarrow \rho_c$.

Similar results are obtained for larger system sizes, as shown in figure 4, for the middle cell of a system of size 15.

3.2. A three-dimensional semi-dispersing billiard table

The second model we consider is a three-dimensional version of the two-dimensional lattice billiard considered above, displayed in figure 5. Each cell is of cubic shape, bordered by cylindrical walls along its edges, with a single spherical particle trapped inside. The two parameters are defined identically to the two-dimensional model, with the bounds $l/2 < \rho < l/\sqrt{2}$ and $\rho_c \equiv \sqrt{\rho^2 - l^2/4} < \rho_m < \rho$, here with $l = 1$. As $\rho_m \rightarrow \rho_c$, we expect the energy exchange dynamics will be accurately described by the stochastic model discussed in section 2 [6]. For the sake of the present investigation, the size of the system was set to three and the walls of the left and rightmost cells were thermalized to unit temperatures. A complete report on the numerical investigations of the billiard dynamics will be the subject of a separate publication [9].

Numerical simulations of this model are reported using $\rho = 1/2$ (for which $\rho_c = 0$)³ and varying ρ_m in the range from 0.20 to 0.49. The expectation values of the energy moments are given, in the three-dimensional canonical ensemble at unit temperature, by $\langle \epsilon^n \rangle = 2^{-n}(2n+1)!!$, which we checked had been accurately reached within three to four digits for the first four moments.

As displayed in the left panel of figure 3(b), the separation of timescales, $\nu_B \ll \nu_W$, becomes effective quite early in the parameter range and, correspondingly, the waiting time distributions are very similar to the waiting time distributions of the corresponding stochastic model, for values of ρ_m as large as 0.3. There is no clear evidence that the scaling law departs from the algebraic law with exponent 10, but this is expected in view of the results presented for the three-dimensional stochastic model in the right panels

² Here and below the histograms were divided up into 400 bins, spanning times up to 20 times the observed mean waiting time, recording up to 10^8 events. The vertical and horizontal scales on these distributions were chosen so that the distributions be normalized, with a mean waiting time of unity.

³ This choice of ρ is the lower bound of its range of possible values; it corresponds to the limiting case where opposite cylinders of radius ρ do not overlap but rather are tangent and form cusps. The moving particles remain trapped inside the cells even as their radius $\rho_m \rightarrow 0$ and are able to exchange energies with neighbouring particles for all strictly positive values of their radius.

Waiting time distributions of confined particle systems with rare interactions

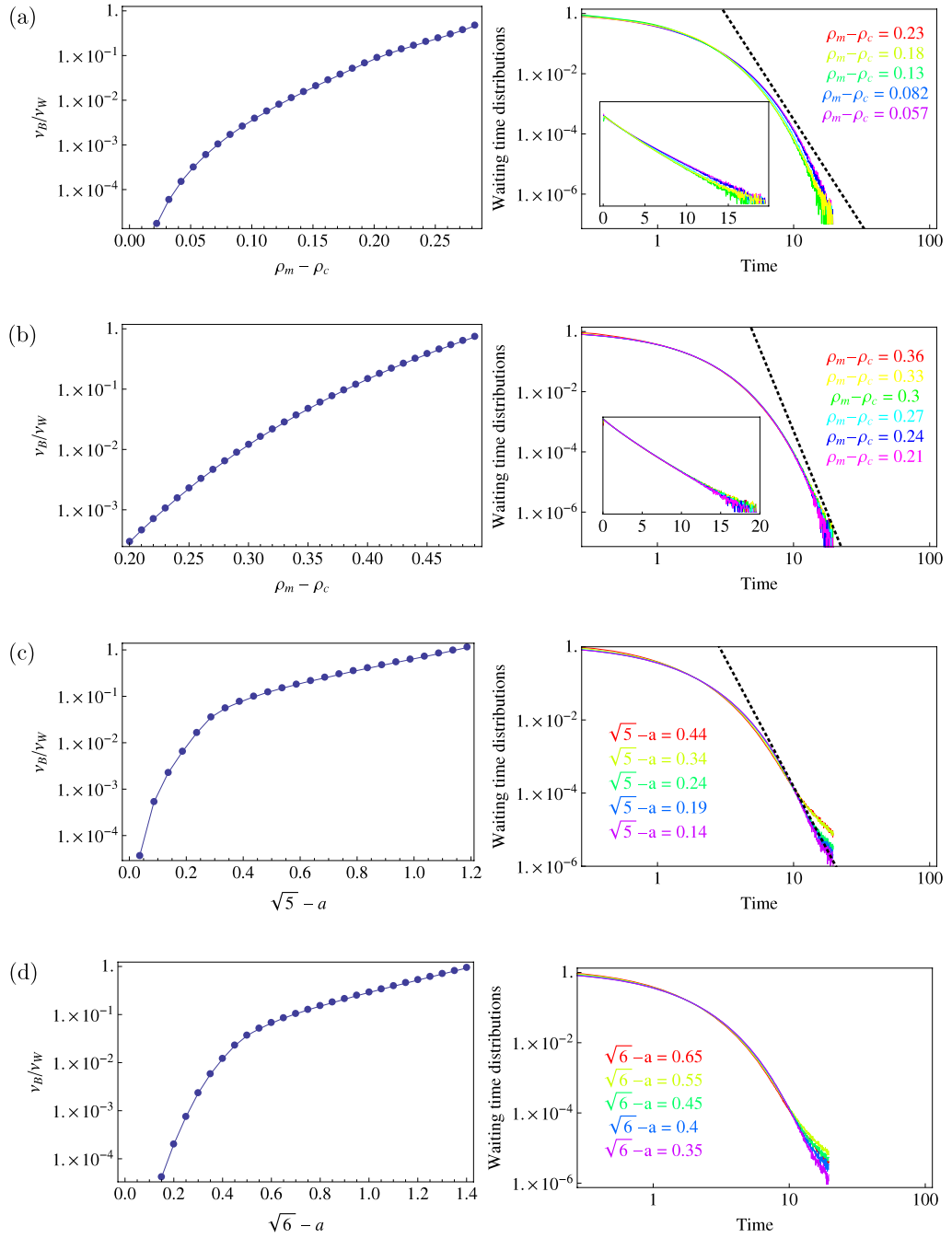


Figure 3. Left panels: ratio of frequencies of binary collisions and wall collisions. Right panels: waiting time distributions. The four sets of figures correspond to the four billiard models considered in the text. (a) 2D dispersing lattice billiard; (b) 3D semi-dispersing lattice billiard; (c) square-strings model; (d) cube-strings model. Notice that the vertical and horizontal scales were chosen so that the distributions are normalized to unity, with mean waiting time of unity. For the sake of comparison, thick dotted black lines are shown with an algebraic exponent -7 in (a), (c) and (d), and -10 in (b). The insets in (a) and (b) are on semi-log scales, with the same vertical scales as in the outer figures.

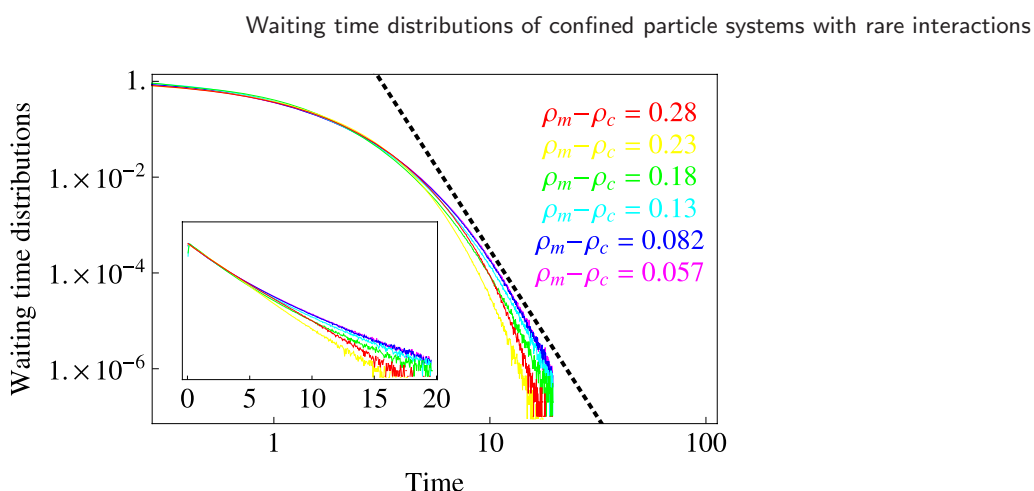


Figure 4. Numerical computation of the waiting time distribution of the two-dimensional lattice billiard, computed for the middle cell of a system of size 15 and several values of the parameter ρ_m , with the walls of cells 1 and 15 thermalized to unit temperatures. Notice that the last two curves superimpose. Thus, even though larger statistics would be desirable, the decay clearly appears to be faster than the algebraic tail exponent seven (thick dotted line), even as the parameter tends to its critical value, $\rho_m \rightarrow \rho_c$.

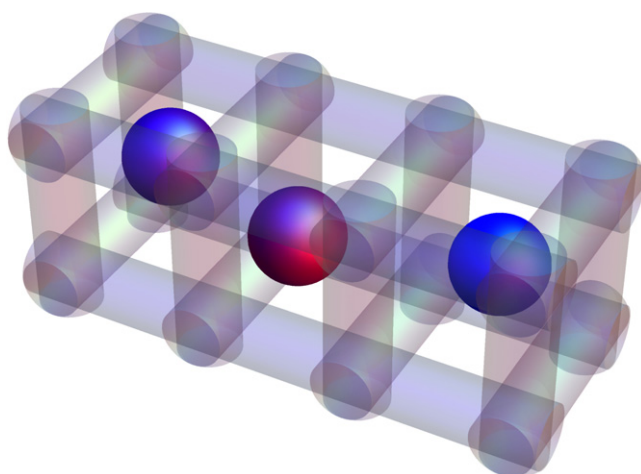


Figure 5. Three-dimensional lattice billiard with cubic cells and cylindrical edges. Here again the walls of the left and rightmost cells are thermalized to unit temperatures.

of figure 1. Ten to hundred times larger statistics would be needed to reach a definite conclusion, which is hardly justifiable.

3.3. Two- and three-dimensional semi-defocusing billiard tables

The third and fourth models we investigate are models of particles trapped within polygonal billiard cells of two and three dimensions, respectively, in the form of squares or cubes of side length unity. Interactions are mediated through massless strings that join

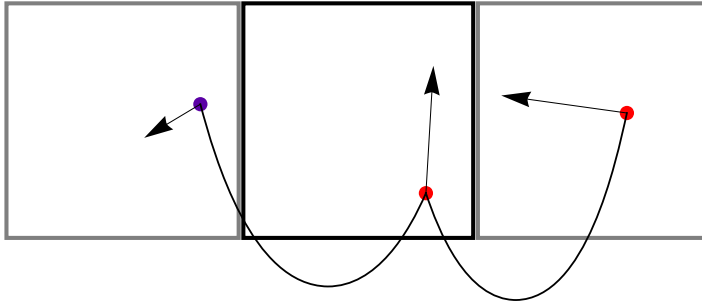


Figure 6. Three-cell square-strings model with thermalized walls in the left and right cells (grey walls). The point particles carry a certain amount of kinetic energy, which they can partially exchange through binary collision events, which occur when the distance between two neighbouring particles reaches a maximal bound a .

pairs of neighbouring particles. Two particles that are joined by a string thus move freely until they reach a mutual distance a , at which point the string becomes taut and exerts an instantaneous impulse on each particle, which interchanges the velocity components along the longitudinal direction. Both these models are examples of higher-dimensional semi-defocusing billiards, whose dynamics were investigated in [10]. The two-dimensional model, depicted in figure 6, is referred to as the square-strings model [3]. By extension, the three-dimensional model will be referred to as the cube-strings model; it is very similar to the square-strings model, except for the dimensionality of the trapping cells.

The models' parameter a takes values in the interval $1 < a < \sqrt{5}$ in the case of the two-dimensional square cells, corresponding to frequent interactions when the parameter is close to 1, and rare when it is close to $\sqrt{5}$, the length of the diagonal of the rectangle formed by two neighbouring squares. Similarly, in the case of three-dimensional cubic cells, the parameter takes values in the interval $1 < a < \sqrt{6}$.

The peculiarity of these two models, compared to the previous ones, is that the dynamics inside the polygons do not mix the velocity angles; it is typically ergodic, but only with respect to the distribution of positions of a particle along the surface of the cells. The models are still chaotic, but only as a result of the interactions between the neighbouring particles. As a consequence, even in the limit of rare interactions, the evolution of the local energy variables is not easily amenable to a stochastic process described by a master equation of the type studied in section 2. Nevertheless, it was shown in [3] that in the limit where the interactions become rare—so that individual particles typically rattle ergodically about their respective cells over large time intervals before they exchange energy—the heat conductivity of this model can be computed from a Boltzmann equation which assumes an effective factorization of the phase-space distribution of the system over the individual cells. As in the models discussed in sections 3.1 and 3.2, the heat conductivity is then simply given in terms of the frequency of energy exchanges (up to a dimensional constant), which is well corroborated by numerical computations.

Numerical computations of these two models are here reported for systems of three cells, with left and rightmost cells thermalized to unit temperatures. The parameters were varied from $a = 1.05$ to 2.20 for the square-strings model and from $a = 1.05$ to 2.30

for the cube-strings model. The accuracy of the thermalization, whether in the two- or three-dimensional canonical ensemble, was checked throughout the range of parameter values to three digits of accuracy.

The numerical computations of the waiting times statistics are shown in figures 3(c) and (d) for the two-dimensional and three-dimensional cells, respectively. In both cases, as the interactions become rarer, the distributions are found to develop algebraic tails with exponents close to seven. This behaviour persists when the system size is increased. Whether seven is indeed the algebraic tail exponent of the waiting time distributions of these two models requires further investigation and should not be interpreted as a vindication of equation (8); a different approach is needed. In view of the cylindrical structure of these models, which is described at length in [10], particles can rattle around their cells for a very long time until a collision eventually occurs. Mixing can therefore be slow and algebraic tails of the waiting time distributions are thus expectable.

4. Conclusions

The observation by the authors of [1] that the thermodynamic potential describing the macroscopic fluctuations of the current and local energies of a class of locally confined particle systems may be neither analytic nor strictly convex relies on the assumption that their waiting time distributions have algebraic tails. In this respect, whether the corresponding exponent differs from their prediction would have little consequence on the validity of their observation. Our results, however, indicate the algebraic decay of the waiting time distributions is borne out by a restricted class of models only, much narrower than had been contemplated.

Through several examples of systems of particles confined to separate cells, and which are allowed to exchange energy on arbitrary long timescales, we have provided evidence that the waiting time distributions of systems of gas particles confined inside an inert nanoporous matrix fall off faster than predicted by our naive dimensional predictions, based on stochastic energy exchange models. Our results emphasize the important role played by the chaoticity of the confining dynamics in removing the algebraic tails of these distributions.

Though our models were restricted to a single particle per trap, it should be clear this is not a restriction. In fact, similar results are expected when many particles are allowed to interact within each cell, since the interaction among particles trapped in the same cell typically mixes local phase-space coordinates, and also when particles are allowed to hop from cell to cell through the nanopores, which the models studied here were specifically designed to prevent.

We conclude by reiterating the crucial role the dimensionality of the underlying dynamics plays when it comes to randomising the amount of energy exchanged through successive interactions. It will be interesting to further investigate the possibility of an algebraic decay of the waiting time distributions in models whose confining dynamics is unable to efficiently mix the local phase-space coordinates. Heavy-tailed distributions are, however, unlikely to prevail in the presence of locally mixing dynamics in higher dimensions [11].

Acknowledgments

The author acknowledges useful discussions with P Gaspard, R Lefevere and L Zambotti. He also wishes to thank M Lenci for comments. This work benefited from financial support by the Belgian Federal Government under the Inter-university Attraction Pole project NOSY P06/02. The author is financially supported by the Fonds de la Recherche Scientifique F.R.S.-FNRS.

References

- [1] Lefevere R, Mariani M and Zambotti L, *Macroscopic fluctuation theory of aerogel dynamics*, 2010 *J. Stat. Mech.* [L12004](#)
- [2] Gaspard P and Gilbert T, *Heat conduction and Fourier's law by consecutive local mixing and thermalization*, 2008 *Phys. Rev. Lett.* **101** 020601
- [3] Gilbert T and Lefevere L, *Heat conductivity from molecular chaos hypothesis in locally confined billiard systems*, 2008 *Phys. Rev. Lett.* **101** 200601
- [4] Gaspard P and Gilbert T, *Heat conduction and Fourier's law in a class of many particle dispersing billiards*, 2008 *New J. Phys.* **10** 3004
- [5] Gaspard P and Gilbert T, *On the derivation of Fourier's law in stochastic energy exchange systems*, 2008 *J. Stat. Mech.* [P11021](#)
- [6] Gaspard P and Gilbert T, *Heat transport in stochastic energy exchange models of locally confined hard spheres*, 2009 *J. Stat. Mech.* [P08020](#)
- [7] Tehver R, Toigo F, Koplik J and Banavar J R, *Thermal walls in computer simulations*, 1998 *Phys. Rev. E* **57** 17
- [8] Chernov N, *Entropy, Lyapunov exponents, and mean free path for billiards*, 1997 *J. Stat. Phys.* **88** 1
- [9] Gilbert T, unpublished
- [10] Gilbert T and Sanders D P, *Stable and unstable regimes in higher-dimensional convex billiards with cylindrical shape*, 2011 *New J. Phys.* **13** 023040
- [11] Saussol B, *On fluctuations and the exponential statistics of return times*, 2001 *Nonlinearity* **14** 179